Dispersion of electrostatic surface plasmons

W. L. Schaich
Physics Department, Indiana University, Bloomington, Indiana 47405
(Received 21 October 1996)

Calculations of the surface plasmon dispersion are presented for a series of models with the same bulk density, but different surface conditions. The results extend out to surface wave vectors as large as 0.3 times the Fermi wave vector and are generally nonlinear in shape. [S0163-1829(97)04315-4]

There has recently been considerable progress in understanding surface collective modes on metals. Experiment and theory have been successfully applied to simple metals to clearly establish the existence and dispersion of surface plasmons.[1–4] Much of the conceptual and computational progress is due to the d-parameter formalism, whose utility in the context of metal surfaces was developed by Feibelman.[5] As applied to systems where band structure effects may be ignored, this approach derives the initial dispersion of the (monopole) surface plasmon in the electrostatic limit as[5–7]

$$\omega_s^2=\frac{1}{2}\omega_B^2[1+Qd(\omega_s)+\cdots], \tag{1}$$

where $\omega_B^2=4\pi n_B e^2/m$ is the bulk plasmon frequency, Q is the mode's wave vector parallel to the surface, and the d parameter is to be found from

$$d(\omega_s)=\int dx\, x\,\delta\rho(x;\mathbf{Q}=0;\omega_s)\Big/\int dx\,\delta\rho(x;\mathbf{Q}=0,\omega_s), \tag{2}$$

with $\delta\rho(x;\mathbf{Q}=0,\omega_s)$ the induced density profile due to a weak, spatially uniform electric field applied along the surface normal at frequency ω_s. Thus both the sign and magnitude of the initial dispersion with Q are set by $d(\omega_s)$, which historically has been the focus of attention.

In writing Eqs. (1) and (2) we have assumed that the bulk metal, where the electron density tends to n_B, lies towards positive x. The location of $x=0$ is where the equilibrium electron density would stop if there were no allowance for tunneling out into vacuum or for Friedel oscillations back into the interior. With these choices one can see that if the centroid of $\delta\rho$ lies ''outside'' the metal (in $x<0$) then the surface plasmon will initially disperse downward with Q. Conversely, if the centroid lies inside, the initial dispersion is upward.

The recent experiments on simple metals clearly show that the initial dispersion is downward, and calculations on the *best* models of a neutral jellium surface are consistent with these observations. We emphasize *best* here because the value of d is known to be quite sensitive to subtle changes in the model description. For instance, for a simple hydrodynamic or infinite barrier model, $\mathrm{Re}d(\omega_s)$ is strongly positive.[8,9]

In this paper we examine whether this model sensitivity of the surface plasmon dispersion persists when one considers higher-Q values, beyond the range where Eq. (1) applies. At the same time we investigate how quickly higher-order terms in Q become important in Eq. (1). The theoretical derivations that lead to Eq. (1) discard such corrections at several stages without making quantitative estimates of their size,[5–7,10–12] so our specific calculations should allow more explicit constraints on the validity limit of Eq. (1).

The scheme we use to determine the surface plasmon energy at a given $\mathbf{Q}$ is to look for a peak in the imaginary part of the reflection amplitude as a function of frequency. Since we consider only $Q\gg\omega_B/c$, where c is the speed of light, we can use electrostatics rather than electrodynamics to describe the reflection process. With an applied potential of the form $\varphi_A e^{-Qx}e^{i(\mathbf{Q}\cdot\mathbf{X}-\omega t)}$, where the two-dimensional vectors $\mathbf{X}$ and $\mathbf{Q}$ lie in the surface plane, the reflection amplitude $r(\mathbf{Q},\omega)$ is defined by

$$r=\frac{2\pi}{Q}\int dx e^{-Qx}\delta\rho(x;\mathbf{Q},\omega)/\varphi_A, \tag{3}$$

where $\delta\rho$ is the (linearly) induced charge density. In turn $\delta\rho$ is formally determined by

$$\delta\rho(x;\mathbf{Q},\omega)/\varphi_A=\int dx'\,\chi(x,x';\mathbf{Q},\omega)e^{-Qx'}, \tag{4}$$

where the density response function χ for the interacting electrons will be calculated using a mean-field approximation from the analogous quantity χ_0 for noninteracting electrons. This requires the solution of the integral equation

$$\chi(x,x')=\chi_0(x,x')+\int d\overline{x}\int d\overline{x'}\,\chi_0(x,\overline{x})v_{\mathrm{eff}}(\overline{x,x'})\chi(\overline{x'},x'). \tag{5}$$

The effective interaction that appears here in general has separate contributions from a direct Hartree term and from a local-density functional approximation (LDA) for exchange and correlation effects:

$$v_{\mathrm{eff}}(x,x';\mathbf{Q},\omega)=\frac{2\pi}{Q}e^{-Q|x-x'|}+v_{\mathrm{xc}}(x)\,\delta(x-x'), \tag{6}$$

where

$$v_{\mathrm{xc}}(x)=\left.\frac{\partial^2[n\epsilon_{\mathrm{xc}}(n)]}{e^2\partial n^2}\right|_{n=n_0(x)}, \tag{7}$$

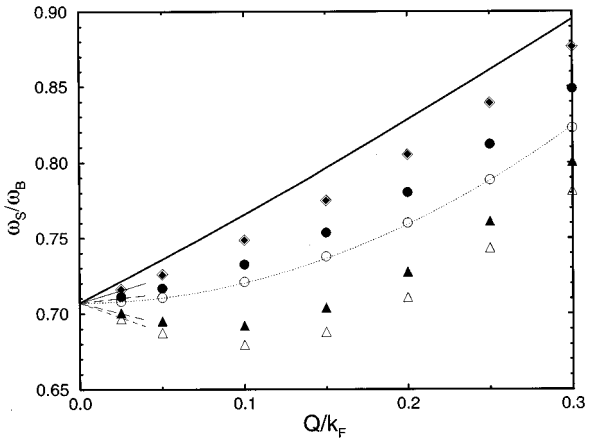

FIG. 1. Surface plasma frequency ω_s versus surface wave vector Q. The former is normalized by the bulk plasmon frequency ω_B and the latter by the Fermi wave vector k_F. The solid curve is from a hydrodynamic calculation. The diamonds are from infinite barrier calculations, done in either real space (open diamonds) or Fourier space (filled diamonds). The circles and triangles are from calculations for non-neutral and neutral jellium models, respectively. Within these models the open (filled) symbols plot RPA (LDA) results. At small Q we show the initial slope of the surface plasmon as calculated from d parameter theory. The thin solid line is for the infinite barrier model. The long-dashed lines are RPA results for self-consistent barriers, while the short-dashed lines are LDA results for the same barriers. For the non-neutral jellium model we also show a fit to Eq. (9) determined by minimizing the mean-square deviation over the whole Q range.

with $\epsilon_{\rm xc}$ the exchange-correlation energy per electron for a uniform electron gas of density n and $n_0(x)$ the ground-state density profile of our semi-infinite system. For a self-consistent calculation the same $\epsilon_{\rm xc}$ must be used in determining $n_0(x)$, via a Lang-Kohn calculation of the ground state.[13] We refer to the full implementation of the above scheme as a LDA calculation. If the second term in Eq. (6) is omitted in the solution of Eq. (5), then we label the results as RPA (random-phase approximation).

A summary of our numerical results is given in Fig. 1. All the calculations have been done for systems with a common bulk density, described by an r_s parameter equal to 2.16, and use a small *ad hoc* damping determined by replacing $\omega \rightarrow \omega + i\gamma$ with $\gamma/\omega_B = 0.01$. The choice of these parameters is based on an experimental system realized in a study of an asymmetric parabolic quantum well.[14] The r_s value is close to that for Al. At one extreme the solid curve gives the dispersion according to a (single-step) hydrodynamic model for which an analytic solution is possible:[15]

$$\omega_s^2 = \frac{\omega_B^2 + \beta^2 Q^2}{2} + \frac{1}{2}(2\omega_B^2\beta^2 Q^2 + \beta^4 Q^4)^{1/2}. \qquad (8)$$

Here the spatial dispersion parameter $\beta^2 = \frac{3}{5}v_F^2$ with v_F the Fermi velocity. The dispersion is always upward and nearly linear. At the other extreme is a LDA calculation for a neutral jellium model using the Wigner approximation for $\epsilon_{\rm xc}$. Its dispersion is initially downward, then flattens out, and rises thereafter. The same qualitative features are seen in the earlier calculations for specific alkali metals.[2,3] In between these two extremes appear the results from alternate treatments or models of the surface. Note that in all cases we have ignored the possible existence of additional (multipole) surface plasmons.

Our first calculations were done for an infinite barrier model within which considerable analytic progress can be made.[16] For this case we set up two independent codes, one working in real space[2,3,17,18] and one in Fourier space.[19,20] Each calculates a RPA response and as shown in Fig. 1, they agree very well, down to $Q/k_F = 0.025$. This is a useful comparison because as $Q/k_F \rightarrow 0$ one needs in the real-space code to contend with long-ranged Coulomb interactions whose influence is only suppressed by factors of e^{-Qx}. We have incorporated several numerical tricks suggested by Liebsch[21] to improve the accuracy of our real-space codes as $Q/k_F \rightarrow 0$. In particular we formally impose a bulk cutoff at x_c only for the induced density $\delta\rho$. Thus, when calculating $\delta\rho$ for $x < x_c$ we include through χ_0 the effect of the applied and induced potential in both $x < x_c$ and $x > x_c$. When Q is strictly zero such difficulties can be avoided by subtraction methods since the total induced charge and asymptotic potentials are known exactly.[17,18] Indeed the $Q = 0$ calculation of the d parameter, which controls the initial dispersion, can readily be done with either a real-space or Fourier-space code.[20] For more sophisticated models, the Fourier-space approach becomes much more difficult to evaluate,[12,19] while the real-space approach is scarcely changed. We hence use only the latter method for further calculations.

For the neutral jellium model the two lowest dispersions in Fig. 1 compare LDA and RPA results. There is no qualitative difference between them. The predicted ω_s in RPA is for any Q higher than in LDA. Except for the smallest plotted Q values, we used the same real-space cutoffs and mesh sizes as for the infinite barrier model. To get convergent results below $Q/k_F = 0.05$ we used a bulk cutoff of $k_F x_c = 40$ beyond the jellium edge and a step size of $k_F \Delta x = 0.1$, which together lead (when one allows for the vacuum tail) to a matrix of dimension 521 to be inverted to solve Eq. (5). The d parameters are found from a real-space code that incorporates not only subtraction methods but also the sum rule[17] that relates the dipole moment required in Eq. (2) to an integral whose range is limited to $x < 0$, i.e., to induced densities ''outside'' the bulk of the metal.

The remaining results in Fig. 1 are for a different self-consistent surface barrier, the so-called parabolic barrier model for an embedded (or non-neutral) jellium.[22,23] Physically such a system is created when the positive background charge density (still spatially constant) extends far beyond the range of the neutralizing electrons. The potential-energy barrier confining the electrons then no longer saturates with a finite work function, but instead rises indefinitely. We again use the Wigner approximation for $\epsilon_{\rm xc}$ to calculate the self-consistent ground state and determine the response from a real-space code. Although the equilibrium density profile is only slightly different from that of neutral jellium, the response properties are quite distinct.[14,22–27] The results for ω_s lie roughly midway between those for the neutral jellium and infinite barrier models, with the RPA frequencies always above the LDA. Since the d parameter for the LDA response of a parabolic barrier model is identically zero,[25] the surface

plasmon in this case must begin with a quadratic dispersion. For curiosity we show in Fig. 1 how well our results can be represented by

$$\omega_s = \frac{\omega_B}{\sqrt{2}}(1+\alpha Q^2). \tag{9}$$

This functional form allows a good fit.

Now compare the results for different model surfaces. At small Q where the d parameter controls the initial slope, there are considerable differences. For $Q/k_F \gtrsim 0.2$ there are still significant differences in the size of ω_s, but the group velocity $d\omega_s/dQ$ is always positive and nearly model independent. Note too that in this Q range the sign of Red is no longer relevant for predicting or understanding whether ω_s is above or below $\omega_B/\sqrt{2}$.

Figure 1 summarizes mode locations, but gives no information about excitation efficiency or lifetimes. These aspects also differ considerably between the various surface models and can be illustrated by examining the whole surface spectral function $-\mathrm{Im}r(\mathbf{Q},\omega)$, which is often called $\mathrm{Im}g(\mathbf{Q},\omega)$.[28] Figure 2 shows several cases plotted at fixed Q versus ω. The peak locations for such curves have been collected in Fig. 1, but the peak height and width are also of interest. The local optics curve is based on

$$r = \frac{1-\epsilon}{1+\epsilon}, \tag{10}$$

with $\epsilon = 1-\omega_B^2/(\omega+i\gamma)^2$. It has no spatial dispersion and appears the same at any $\mathbf{Q}$. All the other cases depend on Q to varying degrees. The extra broadening (beyond that due to γ) grows with increasing incoherent coupling of the surface plasmon to electron-hole excitations, i.e., with increasing Landau damping. The hydrodynamic model allows no Landau damping at all, while the infinite barrier and parabolic barrier models have very little and the neutral jellium model much more. These trends correlate well with the corresponding imaginary part of the d parameter at ω_s.

We have only shown $-\mathrm{Im}r$ over a limited range of frequency, where the surface plasmon peak dominates. There are additional, weak structures outside this range. At low frequencies such structure comes from direct excitation of electron-hole pairs. It is absent in the local optics and hydrodynamic model and is largest for the neutral jellium model, which alone has a finite work function (which is equal to $0.35\omega_B$). For neutral jellium the structure is a shoulder in $-\mathrm{Im}r$ at the level of 1.0 for $\omega/\omega_B \approx 0.3$. For the infinite or parabolic barrier models the analogous structure is roughly 10 times smaller. At higher frequencies there is a small structure in all but the local optics case as ω increases past ω_B and bulk plasmons can be excited. This extra peak is always less than 0.2 in height for the parameters used here. Finally, for $Q/k_F = 0.2$, we do not see any structure that would imply the existence of a multipole mode. Only for neutral jellium does Imd show a (weak) multipole peak for our choice of r_s and this structure is probably lost in the tail of the broad monopole surface plasmon at $Q/k_F = 0.2$.

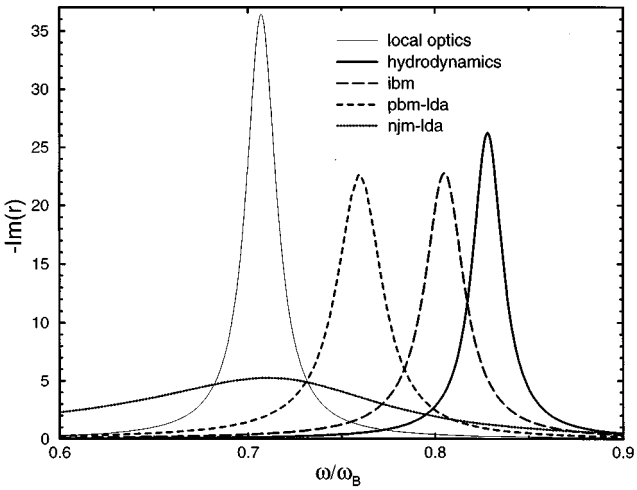

FIG. 2. Surface spectral function $-\mathrm{Im}r(\mathbf{Q},\omega)$ versus frequency ω at fixed wave vector parallel to the surface $\mathbf{Q}$. The magnitude of $\mathbf{Q}$ is $Q/k_F = 0.2$. The different model predictions are plotted on a common scale. The local optics result omits spatial dispersion and peaks at $\omega_B/\sqrt{2}$ for any $\mathbf{Q}$. IBM, PBM, and NJM stand respectively for infinite barrier, parabolic barrier, and neutral jellium models.

Part of the calculations were done on the Cray Research, Inc. Y-MP C90 system at the Pittsburgh Superconducting Center, Pittsburgh. We are grateful to Ansgar Liebsch for several helpful suggestions.

[1] K. D. Tsuei, E. W. Plummer, and P. J. Feibelman, Phys. Rev. Lett. **63**, 2256 (1989).
[2] K. D. Tsuei, E. W. Plummer, A. Liebsch, K. Kempa, and P. Bakshi, Phys. Rev. Lett. **64**, 44 (1990).
[3] K. D. Tsuei, E. W. Plummer, A. Liebsch, E. Pehlke, K. Kempa, and P. Bakshi, Surf. Sci. **247**, 302 (1991).
[4] A. Liebsch, *Electromagnetic Waves: Recent Developments in Research; Vol. 2: Photonic Probes of Surfaces* (Elsevier, New York, 1995).
[5] P. J. Feibelman, Prog. Surf. Sci. **12**, 287 (1982).
[6] J. Harris and A. Griffin, Phys. Lett. **34A**, 51 (1971).
[7] F. Flores and F. Garcia-Moliner, Solid State Commun. **11**, 1295 (1972).
[8] P. Apell, Phys. Scr. **24**, 795 (1981).
[9] W. L. Schaich and K. Kempa, Phys. Scr. **35**, 204 (1987).
[10] D. C. Langreth, Phys. Rev. B **39**, 10 021 (1989).
[11] W. L. Schaich and W. Chen, Phys. Rev. B **39**, 10 714 (1989).
[12] R. R. Gerhardts, *Electromagnetic Waves: Recent Developments in Research; Vol. 1: Spatial Dispersion in Solids and Plasmas* (North-Holland, New York, 1992).
[13] N. D. Lang, Solid State Phys. **28**, 225 (1973).
[14] E. L. Yuh, E. G. Gwinn, P. R. Pinsukanjana, W. L. Schaich, P. F. Hopkins, and A. C. Gossard, Phys. Rev. Lett. **71**, 2126 (1993).
[15] G. Barton, Rep. Prog. Phys. **42**, 963 (1979).
[16] G. W. Ford and W. H. Weber, Phys. Rep. **113**, 195 (1984).
[17] A. Liebsch, Phys. Rev. B **36**, 7378 (1987).
[18] W. L. Schaich, Phys. Rev. B **50**, 17 587 (1994).
[19] K. Kempa and W. L. Schaich, Phys. Rev. B **37**, 6711 (1988).

[20] K. Kempa, A. Liebsch, and W. L. Schaich, Phys. Rev. B **38**, 12 645 (1988).
[21] A. Liebsch (private communication).
[22] J. F. Dobson, Phys. Rev. B **46**, 10 163 (1992).
[23] J. F. Dobson, Aust. J. Phys. **46**, 391 (1993).
[24] W. L. Schaich and J. F. Dobson, Phys. Rev. B **49**, 14 700 (1994).
[25] W. L. Schaich, Surf. Sci. **318**, L1157 (1994).
[26] E. L. Yuh and E. G. Gwinn, Surf. Sci. **305**, 202 (1994).
[27] E. L. Yuh *et al.*, Phys. Rev. B **54**, 11 467 (1996).
[28] B. N. J. Persson and E. Zaremba, Phys. Rev. B **31**, 1863 (1985).